Available online at www.sciencedirect.com
SCIENCE DIRECT®
PERGAMON
Polyhedron 22 (2003) 1865–1870
POLYHEDRON
www.elsevier.com/locate/poly

# Search for new iron single-molecule magnets

Evan M. Rumberger [a], Stephen Hill [b], Rachel S. Edwards [b], Wolfgang Wernsdorfer [c], Lev N. Zakharov [d], Arnold L. Rheingold [d], George Christou [e], David N. Hendrickson [a,*]

[a] Department of Chemistry and Biochemistry – 0358, University of California at San Diego, La Jolla, CA 92093-0358, USA
[b] Department of Physics, University of Florida, Gainesville, FL 32611, USA
[c] Laboratoire Louis-Neél-CNRS, 25 Avenue des Martyrs, 38042 Grenoble Cedex 9, France
[d] Department of Chemistry, University of Delaware, Newark, DE 19716, USA
[e] Department Chemistry, University of Florida, Gainesville, FL 32611-7200, USA

Received 6 October 2002; accepted 14 December 2002

**Abstract**

The synthesis, X-ray structure, and magnetic properties of a trinuclear iron complex with the formulation $[Fe_3O_2Cl_2(4,7\text{-Me-phen})_6](BF_4)_3$ (complex **1**) are reported. DC magnetic susceptibility measurements show the Fe atoms are antiferromagnetically coupled, yielding an $S = 5/2$ ground state. An investigation as to whether complex **1** exhibits the properties associated with single-molecule magnetism was undertaken. Detailed high frequency EPR experiments were carried out to determine the spin Hamiltonian parameters associated with the $S = 5/2$ spin ground state. Analysis of the temperature dependence of the transitions seen with the magnetic field oriented along the easy axis ($z$ axis) of the $Fe_3$ complex confirm that the molecule has a positive $D$ value. A fit of the frequency dependence of the resonances afforded the following spin Hamiltonian parameters: $S = 5/2$, $g_z = 1.95$, $g_x = g_y = 2.00$, $D = 0.844\ cm^{-1}$, $E = \pm 0.117\ cm^{-1}$, and $B_4^0 = -2.7 \times 10^{-4}\ cm^{-1}$. Low temperature magnetization versus magnetic field data confirm that complex **1** has no barrier towards magnetization reversal. Thus, it is concluded that, due to the positive $D$-value, complex **1** is not a single-molecule magnet.


*Keywords:* Single-molecule magnet; Quantum tunneling of magnetization; Nanomagnet; Superparamagnet; Polynuclear iron complex

## 1. Introduction

Polynuclear iron complexes have attracted the interest of researchers for several reasons. From a biological point of view, there has been considerable interest in understanding the iron storage protein ferritin [1]. Dinuclear oxo or hydroxo bridged Fe complexes have been under intense study, for example, as model compounds since this framework is identified to be involved as a cofactor in several metalloproteins [2].

Recently, considerable research has been directed towards the synthesis of high nuclearity transition metal complexes that exhibit single-molecule magnetism [3]. Polynuclear complexes, assembled with certain topologies, may have a high-spin ground state $S$ that, in combination with a *negative* axial type magnetoanisotropy, gives a barrier for magnetization reversal. Each molecule is a single domain nanomagnet. At low enough temperatures, hysteresis in magnetization versus magnetic field may be observed. The most thoroughly studied single-molecule magnet (SMM) is $[Mn_{12}O_{12}(O_2CCH_3)_{16}(H_2O)_4]\cdot 2CH_3COOH\cdot 4H_2O$, called $Mn_{12}Ac$ for short [4,5]. Considerable interest in the study of SMMs was generated with the observation that $Mn_{12}Ac$ reverses its direction of magnetization not only by thermal activation, but also by quantum tunneling of magnetization (QTM) [6,7]. Iron SMMs have been of considerable interest, because it is known that the nuclear spin of the transition metal in a polynuclear SMM affects the rate of QTM. Manganese has a nuclear spin of $I = 5/2$, whereas $^{56}Fe$ has a nuclear spin of $I = 0$. In fact, Gatteschi and co-workers [8] showed that $^{57}Fe$ ($I = 1/2$) enrichment of the polynuclear iron SMM $Fe_8$ has a profound effect on the rate of QTM.

* Corresponding author.
*E-mail address:* dhendrickson@ucsd.edu (D.N. Hendrickson).

0277-5387/03/$ - see front matter © 2003 Elsevier Science Ltd. All rights reserved.
doi:10.1016/S0277-5387(03)00175-X

SMMs that have half-integer spin ground states are predicted [9] to have QTM suppressed in the absence of a magnetic field. Thus, for a SMM with $S = 9/2$, for example, QTM between the $m_s = -9/2$ and $m_s = 9/2$ states should not occur in zero-field, because these two states comprise a Kramers degenerate pair. Only a magnetic field can break the symmetry between the $m_s = -9/2$ and $m_s = 9/2$ states and lead to QTM. Several half-integer spin polynuclear Mn SMMs have been studied [10–15] and, in spite of the above prediction, QTM was observed. This was explained by noting that Mn has a nuclear spin of $I = 5/2$. The nuclear spin of such a polynuclear Mn SMM leads to a small magnetic field, the transverse component of which leads to QTM. Very recently, Wernsdorfer et al. [16] for the first time established the presence of spin-parity dependent tunneling by comparing the transverse field dependence of the tunnel splitting of integer and half-integer spin SMMs.

As a consequence of the above observations, one goal in the area of SMMs is to prepare a half-integer spin SMM consisting of metal ions with no nuclear spin. In this paper we present the results for a $S = 5/2$ $Fe_3$ complex.

## 2. Experimental

### 2.1. Synthesis

All solvents and reagents where used as received, no purification was necessary. All reactions were performed under aerobic conditions.

#### 2.1.1. $[Fe_3O_2Cl_2(4,7\text{-Me-phen})_6](BF_4)_3$ (complex **1**)

To a 75 ml methanol solution of $FeCl_3 \cdot 6H_2O$ (1.00 g, 3.70 mmol) was added with stirring 2-piperdine-methanol (0.852 g, 7.40 mmol) affording an orange–yellow solution. To this solution was added 4,7-dimethylphenanthroline (1.67 g, 7.4 mmol), whereupon the solution immediately turned a deep brick-red color. Addition of sodium tetrafluoroborate (1.21 g, 11.1 mmol) produced no noticeable color change. After 15 min of stirring, a red–brown precipitate slowly formed. This precipitate was collected by filtration and washed with copious amounts of methanol (1.48 g collected, 64% yield based on Fe content). The product analyzed as $1 \cdot 5H_2O$. *Anal.* Calc. (found) for $C_{84}H_{82}B_3Cl_2F_{12}Fe_3N_{12}O_7$: C, 53.9 (52.2); H, 4.41 (4.29); N, 8.98 (8.66)%. Selected IR data ($cm^{-1}$): 3384.6(br); 1621(s); 1521(s); 1421(s); 1066(br); 796(m); 725(m); 646(m); 582(w). Crystals of the formulation $1 \cdot 4MeCN \cdot H_2O$ were grown by slowly diffusing ether vapors into an acetonitrile solution.

### 2.2. Physical measurements

DC magnetic susceptibility data were collected with a Quantum Design MPMS magnetometer equipped with a 5.5 T magnet. Powdered microcrystalline samples were restrained with eicosane to prevent torquing of the crystallites. Pascal's constants [17] were employed to adjust observed magnetic susceptibilities with a diamagnetic correction. High frequency EPR (HFEPR) measurements were performed on home made instrumentation described elsewhere [18]. Low temperature magnetization versus field data were collected using an array of micro-SQUIDs which is described in Ref. [19].

## 3. Results and discussion

### 3.1. Description of structure

Fig. 1 shows an ORTEP illustration of complex **1**. Relevant X-ray crystallography parameters are detailed in Table 1. Complex **1** crystallizes in the monoclinic space group $P2_1/c$. The core can be described as one central Fe atom (Fe2 in Fig. 1) bound to two μ-oxo-Fe (Fe3 and Fe4 in Fig. 1) units resulting in a 'v-shaped' topology. Complex **1** has a pseudo-$C_2$ axis that passes through the Fe2 atom. Iron atoms Fe1 and Fe3 are six coordinate, with each Fe atom bound to four nitrogen atoms of two 4,7-dimethylphenanthroline ligands, one

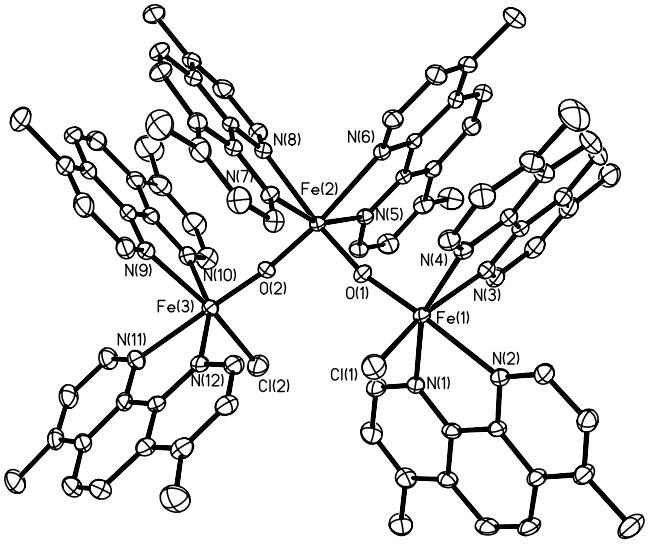


Fig. 1. ORTEP of complex **1**, displayed at the 50% probability level. Hydrogen atoms, solvate molecules, and anions have been omitted for clarity. Selected bond distances (Å) and angles (°): Fe2–O1 1.816, Fe2–O2 1.811, Fe2–N6 2.272, Fe2–N7 2.177, Fe2–N8 2.250, Fe2–N5 2.152, Fe1–O1 1.772, Fe1–Cl1 2.266, Fe1–N1 2.137, Fe1–N2 2.271, Fe1–N3 2.302, Fe1–N4 2.152, Fe3–O2 1.773, Fe3–Cl2 2.289, Fe3–N9 2.217, Fe3–N10 2.150, Fe3–N11 2.249, Fe3–N12 2.139, O2–Fe2–O1 103.04, Fe1–O1–Fe2 166.82, Fe3–O2–Fe2 171.25.

Table 1
Crystal data and structure refinement for complex **1**

| | |
|---|---|
| Empirical formula | C90 H89 B3 Cl2 F12 Fe3 N15 O3 |
| Formula weight | 1927.64 |
| Temperature (K) | 218(2) |
| Wavelength (Å) | 0.71073 |
| Crystal system | monoclinic |
| Space group | $P2_1/c$ |
| Unit cell dimensions | |
| $a$ (Å) | 22.6592(14) |
| $b$ (Å) | 13.0388(8) |
| $c$ (Å) | 29.9777(17) |
| $\alpha$ (°) | 90 |
| $\beta$ (°) | 98.1470(10) |
| $\gamma$ (°) | 90 |
| $V$ (Å$^3$) | 8767.5(9) |
| $Z$ | 4 |
| $D_{calc}$ (Mg m$^{-3}$) | 1.460 |
| Absorption coefficient (mm$^{-1}$) | 0.636 |
| $F(0\,0\,0)$ | 3972 |
| Crystal size (mm) | $0.25 \times 0.20 \times 0.10$ |
| Theta range for data collection | 0.91°–28.33° |
| Index ranges | $-29 \le h \le 30$, $-16 \le k \le 15$, $-39 \le l \le 39$ |
| Reflections collected | 64706 |
| Independent reflections | 21201 [$R_{int} = 0.0594$] |
| Completeness to theta = 28.33° | 97.0% |
| Absorption correction | SADABS |
| Refinement method | Full-matrix least-squares on $F^2$ |
| Data/restraints/parameters | 21201/0/1146 |
| Goodness-of-fit on $F^2$ | 1.046 |
| Final $R$ indices [$I > 2\sigma(I)$] | $R_1 = 0.0825$, $wR_2 = 0.1918$ |
| $R$ indices (all data) | $R_1 = 0.1295$, $wR_2 = 0.2161$ |
| Largest difference peak and hole (e Å$^{-3}$) | 0.893 and −0.804 |

chlorine atom, and one μ-oxide. The central Fe is bound to four nitrogen atoms of two 4,7-dimethylphenanthroline ligand and two μ-oxides. The asymmetric unit contains one Fe trinuclear moiety and three disordered tetrafluoroborate anions. Complex **1** crystallized with one water and four acetonitrile solvate molecules. One of the 4,7-dimethylphenanthroline ligands coordinated to each terminal Fe atom exhibits a short contact distance of 3.418 Å to one 4,7-dimethylphenanthroline ligand coordinated to the central Fe atom, indicating that there may be intramolecular π–π interactions; see the figure caption for relevant bond distances and angles.

### 3.2. DC magnetic susceptibility studies

Fig. 2 illustrates the variable-temperature magnetic susceptibility data measured from 300 K down to 5 K with an applied field of 1 T. Upon cooling, the value of $\chi_M T$ decreases from 4.35 cm$^3$ K mol$^{-1}$ at 300 K to a plateau value of 4.10 cm$^3$ K mol$^{-1}$ at 50 K, whereupon below 15 K it sharply decreases to a value of 3.91 cm$^3$ K mol$^{-1}$ at 5 K. These data are consistent with an antiferromagnetically coupled Fe(III)$_3$ unit having an

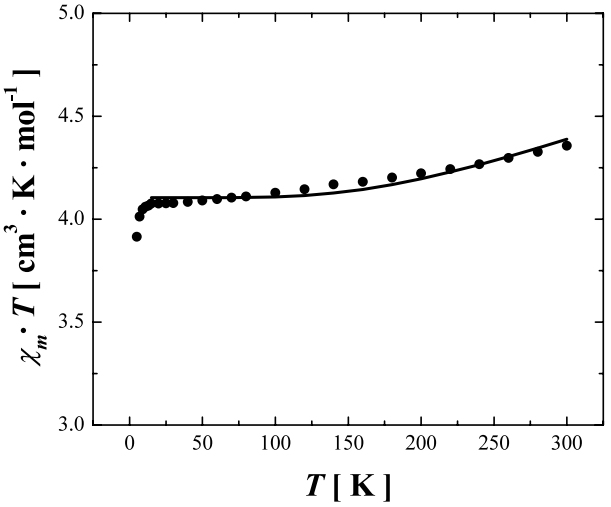


Fig. 2. Plot of $\chi_M T$ versus temperature where $\chi_M$ is the molar susceptibility. The solid line represents the best least-squares fit of the data, see the text for details.

$S = 5/2$ ground state. The sharp decrease below 15 K is due to zero-field splitting. The solid line in Fig. 2 represents the best fit of the data to the Hamiltonian:

$$H = -2J[\hat{S}_1\hat{S}_2 + \hat{S}_2\hat{S}_3] - 2J'\hat{S}_1\hat{S}_3 \quad (1)$$

where the quantity $J$ takes into account the exchange interaction between the central and terminal Fe atoms and the parameter $J'$ gauges the exchange interaction between the two terminal Fe atoms. A best fit was obtained with the parameters $g = 1.95$, $J = -66.5$ cm$^{-1}$, and $J' = 12.5$ cm$^{-1}$. It was not possible to obtain an acceptable fit to the data if the $J'$ parameter was excluded.

The nature of the spin ground state of complex **1** was probed further by measuring the reduced magnetization at several magnetic fields. Fig. 3 shows the data collected at four different fields and several temperatures. Full matrix diagonalization (employing a powder average) of the spin Hamiltonian describing an $S = 5/2$ ground state including the Zeeman interaction and second order zero-field splitting, $D(\hat{S}_z^2)$, was used to obtain a least-squares fit to the data. No global minimum was found, however, two sets of spin Hamiltonian parameters could satisfactorily fit the experimental data, one set in which the $D$-value was positive ($g = 1.94$, $D = 1.1$ cm$^{-1}$) and one in which the $D$-value was negative ($g = 1.95$, $D = -0.9$ cm$^{-1}$). It is clear, despite the ambiguity in the sign of the $D$-value, that complex **1** possesses appreciable magnetoanisotropy in the ground state, as indicated by the non-superimposable isofield reduced magnetization versus $H/T$ curves obtained at several different magnetic fields in the 2.0–4.0 K range.

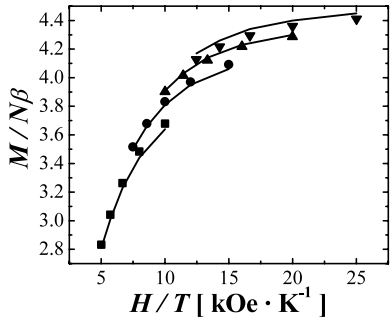


Fig. 3. Plot of the reduced magnetization ($M/N\beta$) where $M$ is the molar magnetization, $N$ is Avogadro's number, and $\beta$ is the Bohr magneton, plotted versus $H/T$. Data were collected at 5 (▼), 4 (▲), 3 (●), and 2 T (■) in the temperature range of 2.0–4.0 K. The solid line represents the least-squares fit of the data with the parameters $S = 5/2$, $g = 1.94$, $D = 1.1$ cm$^{-1}$. See the text for the details of this analysis.

### 3.3. High frequency EPR (HFEPR) studies

In order to definitively determine the spin Hamiltonian parameters, HFEPR data of a powdered sample of complex **1** were collected. In Fig. 4 are shown the HFEPR spectra of complex **1** collected with a frequency of 131.878 GHz and at temperatures of 1.36, 5, 10, and 14 K. At each temperature, a very complex spectrum was obtained. Resonances corresponding to the ground state were identified as those that persisted at the lowest temperatures (labeled $z_1$, $z_2$, $z_3$, $x_1$, and $y_1$). Several peaks are observed below 2 T that correspond to level mixing. Upon raising the temperature, the appearance of strong $z_2$ and $z_3$ resonances can be seen. Very sharp peaks also emerge close to the $x_1$ resonance. These correspond to excited state transitions. Thus, the closely spaced resonances observed in the 2–4 T region correspond to $x$ (or $y$) resonances, and the widely, evenly spaced ones to $z$ resonances. It is concluded that $D$ is in fact positive; for negative $D$, the strongest $z$ resonance would be at the lowest field with the resonances getting weaker with increasing field.

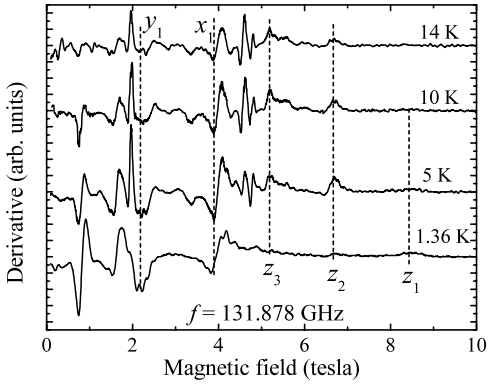


Fig. 4. HFEPR spectra measured at 131.878 GHz for a powdered sample of complex **1**. Data were collected at the temperatures of 1.36, 5, 10, and 14 K. The labeled resonances ($x_1$, $y_1$, $z_1$) were identified as those corresponding to the ground state. Resonances labeled ($z_2$, $z_3$) were identified as excited state transitions within the $S = 5/2$ multiplet.

In Fig. 5 are shown HFEPR spectra obtained for complex **1** collected at 1.36 K with the frequencies of 114.5017, 131.878, 154.0, and 159.489 GHz. After the resonances were identified that are associated with the ground state, the frequency dependence was fit to a $S = 5/2$ spin Hamiltonian. Zeman interactions, including axial zero-field splitting, $D(\hat{S}_z^2)$, rhombicity, $E(\hat{S}_x^2 - \hat{S}_y^2)$, and the fourth order zero-field term $B_4^0\hat{O}_4^0$ were included in the analysis. Fig. 6 depicts the results obtained from the fit for the $z$ resonances. Figs. 7 and 8 show the results obtained from the fit of the $x$ and $y$ resonances. For the $x$ and $y$ resonances, only one strong peak was identified. The fits are consistent with a single set of parameters: $g_z = 1.95$, $g_x = g_y = 2$, $D = 0.844$ cm$^{-1}$, $E = \pm 0.117$ cm$^{-1}$, and $B_4^0 = -2.7 \times 10^{-4}$ cm$^{-1}$. Unfortunately, from these parameters it is anticipated that complex **1** is not a SMM. The $D$-value is probably large enough, but it has the wrong sign for complex **1** to exhibit single-molecule magnetism.

## 4. Magnetization versus magnetic field hysteresis

Probably the only way to definitively establish whether the $Fe_3$ complex **1** is a SMM is to determine whether there is hysteresis in the magnetization versus magnetic field response. It is best to carry out magnetization measurements on a single crystal employing a micro-SQUID array [19]. Fig. 9 shows the results of such a determination. A single crystal of complex **1** was mounted on a micro-SQUID array and measurements were carried out to determine the easy axis direction. With the magnetic field oriented along the easy axis, magnetization data were collected as the magnetic field was ramped from −1.2 to +1.2 T. Several different scan rates were used in the temperature region of 0.9–0.040 K. As can be seen in Fig. 9, a single crystal of complex **1**

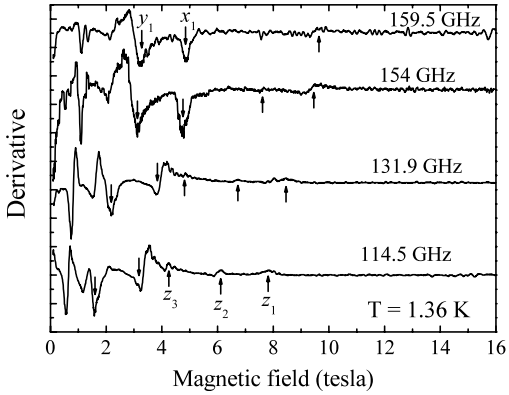


Fig. 5. HFEPR spectra measured at 1.36 K for a powdered sample of complex **1**. Data were collected at the frequencies of 114.5017, 131.878, 150.0, and 159.489 GHz.

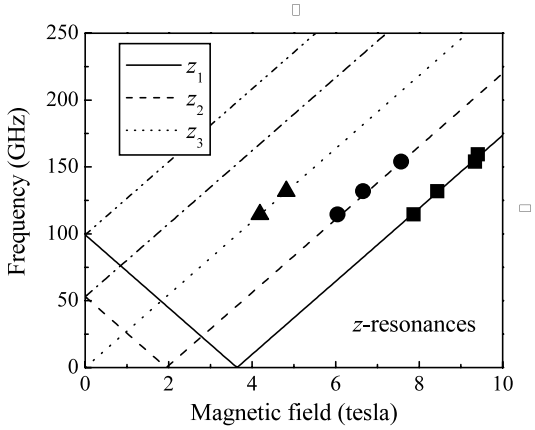


Fig. 6. Zeeman diagram of the spin Hamiltonian associated with the $S = 5/2$ ground state of complex **1** with the magnetic field oriented in the $z$ (easy axis) direction. The solid lines represent the energy spectrum obtained from a best fit of the $z$ resonances.

does not exhibit hysteresis in the plot of magnetization versus magnetic field. The only effects seen are attributable to a phonon bottleneck [20].

It can be concluded that complex **1** is not a SMM. This agrees with the HFEPR data that show $D > 0$. It is necessary to change the sign of the axial zero-field splitting in the $S = 5/2$ ground state of complex **1**. This is not an easy task, for the analysis of the sign and magnitude of a $D$-value for a polynuclear Fe complex is not simple [21].

## 5. Conclusion

The synthesis and crystal structure of a trinuclear Fe complex are reported. Detailed low temperature magnetometry experiments confirm that this complex has no barrier towards magnetization reversal and is thus not a SMM. HFEPR data collected on this sample confirm the lack of an energy barrier since the $D$-value was unambiguously determined to be positive.

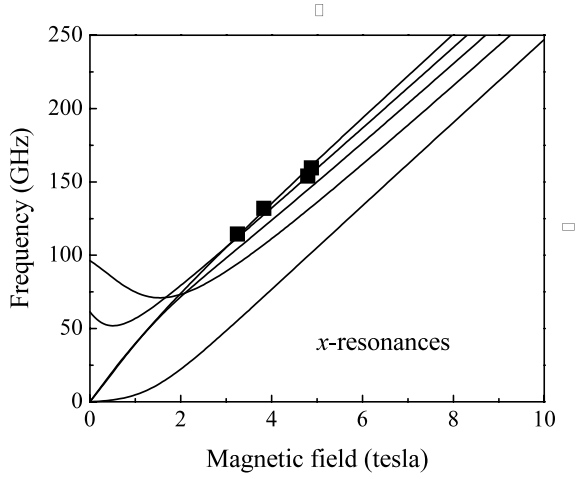


Fig. 7. Zeeman diagram of the spin Hamiltonian associated with the $S = 5/2$ ground state of complex **1** with the magnetic field oriented in the $x$ direction. The solid lines represent the energy spectrum obtained from a best fit of the $x$ resonances.

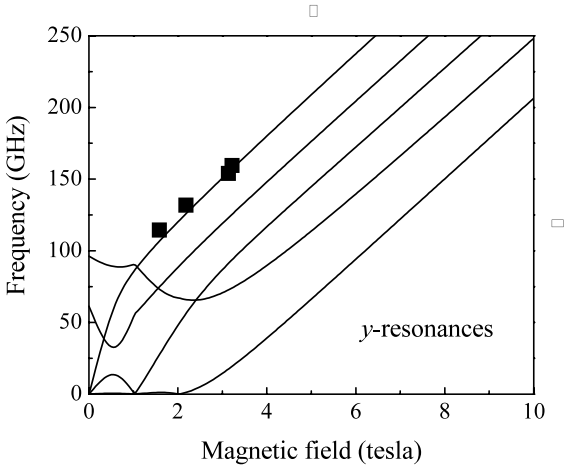


Fig. 8. Zeeman diagram of the spin Hamiltonian associated with the $S = 5/2$ ground state of complex **1** with the magnetic field oriented in the $y$ direction. The solid lines represent the energy spectrum obtained from a best fit of the $y$ resonances.

## 6. Supplementary materials

Crystallographic data for the structural analysis have been deposited with the Cambridge Crystallographic Data Center, CCDC No. 198374. Copies of this information may be obtained free of charge from The Director, CCDC, 12 Union Road, Cambridge, CB2 1EZ, UK (fax: +44-1223-336033; email deposit@ccdc.cam.ac.uk or http://www.ccdc.cam.ac.uk).

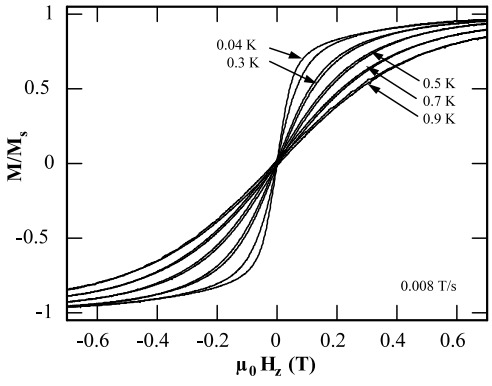


Fig. 9. Plot of the normalized ($M/M_s$) magnetization versus magnetic field ($\mu_0 H$), where $M_s$ is the saturation magnetization. The magnetic field is oriented parallel to the easy axis. Data were collected on a single crystal in the temperature range of 0.9–0.04 K with a scanning rate of 0.008 T $s^{-1}$.

## Acknowledgements

This work was supported by the National Science Foundation.

## References

[1] (a) E.C. Theil, Annu. Rev. Biochem. 56 (1987) 289 (and references therein);
(b) B. Xu, D. Chasteen, J. Biol. Chem. 266 (1991) 19965.
[2] (a) A.L. Feig, S.J. Lippard, Chem. Rev. 94 (1994) 759 (and references therein);
(b) P. Nordlund, H. Eklund, Curr. Opin. Struct. Biol. 5 (1995) 758.
[3] G. Christou, D. Gatteschi, D.N. Hendrickson, R. Sessoli, MRS Bull. 25 (2000) 66.
[4] R. Sessoli, H.-L. Tsai, A.R. Schake, S. Wang, J.B. Vincent, K. Folting, D. Gatteschi, G. Christou, D.N. Hendrickson, J. Am. Chem. Soc. 115 (1993) 1804.
[5] R. Sessoli, D. Gatteschi, A. Caneschi, M.A. Novak, Nature 365 (2000) 141.
[6] J.R. Friedman, M.P. Sarachik, J. Tejada, J. Maciejewski, R. Ziolo, J. Appl. Phys. 79 (1996) 6031.
[7] J.R. Friedman, M.P. Sarachik, J. Tejada, R. Ziolo, Phys. Rev. Lett. 76 (1996) 3830.
[8] R. Sessoli, A. Caneschi, D. Gatteschi, L. Sorace, A. Cornia, W. Wernsdorfer, J. Magn. Magn. Mater. 226 (2001) 1954.
[9] (a) D. Loss, D.P. Di Vincenzo, G. Grinstein, D. Awschalom, J.F. Smyth, Phys. B 189 (1993) 189;
(b) D.P. Di Vincenzo, Phys. B 197 (1994) 109.
[10] S.M.J. Aubin, S. Spagna, H.J. Eppley, R.E. Sager, G. Christou, D.N. Hendrickson, Chem. Commun. 7 (1998) 803.
[11] W. Wernsdorfer, N. Aliaga-Alcade, D.N. Hendrickson, G. Christou, Nature 416 (2002) 406.
[12] S.M.J. Aubin, N.R. Dilley, L. Pardi, J. Krzystek, M.W. Wemple, L.-C. Brunel, M.B. Maple, G. Christou, D.N. Hendrickson, J. Am. Chem. Soc. 120 (1998) 4991.
[13] M. Soler, S.K. Chandra, D. Ruiz, J.C. Huffman, D.N. Hendrickson, G. Christou, Polyhedron 20 (2001) 1279.
[14] S.M.J. Aubin, Z. Sun, L. Pardi, J. Krzystek, K. Folting, L.-C. Brunel, A.L. Rheingold, G. Christou, D.N. Hendrickson, Inorg. Chem. 38 (1999) 5329.
[15] F.L. Mettes, G. Aromi, F. Luis, M. Evangelisti, G. Christou, D.N. Hendrickson, L.J. de Jongh, Polyhedron 20 (2001) 1459.
[16] W. Wernsdorfer, S. Bhaduri, C. Boskovic, G. Christou, D.N. Hendrickson, Phys. Rev. B 6518 (2002) U35.
[17] O. Kahn, Molecular Magnetism, VCH Publishers Inc, New York, 1993.
[18] M. Mola, S. Hill, P. Goy, M. Gros, Rev. Sci. Instrum. 71 (2000) 186.
[19] W. Wernsdorfer, Adv. Chem. Phys. 118 (2001) 99.
[20] I. Chiorescu, W. Wernsdorfer, A. Müller, H. Bögge, B. Barbara, Phys. Rev. Lett. 84 (2000) 3454.
[21] D. Gatteschi, L. Sorace, J. Solid State Chem. 159 (2001) 253.